SUPERVISED AND UNSUPERVISED CONDITION MONITORING OF NON-STATIONARY ACOUSTIC EMISSION SIGNALS

Sigurdur Sigurdsson, Niels Henrik Pontoppidan and Jan Larsen

Informatics and Mathematical Modelling, Richard Petersens Plads,
Technical University of Denmark, 2800 Lyngby, Denmark.
{siggi,nhp,jl}@imm.dtu.dk, Tel +45 4525 3290, Fax +45 4587 2599

ABSTRACT

We are pursuing a system that monitors the engine condition under multiple load settings, i.e. under non-stationary operating conditions. The running speed when data acquired under simulated marine conditions (different load settings on the propeller curve) was in the range from approximately 70 to 125 rotations per minute; furthermore the running speed was stable within periods of fixed load. Electronically controlled engines can change the angular timing of certain events, such as fuel injection in order to optimize its performance. However, this behaviour makes it difficult to detect condition changes across load changes. In this paper we approach this load interpolation problem with supervised and unsupervised learning, i.e. model with normal and fault examples and normal examples only, respectively. We apply non-linear methods for the learning of engine condition changes. Both approaches perform well, which indicates that unsupervised models, modelled without faulty data, may be used for accurate condition monitoring.

KEYWORDS

Signal processing, non-stationary condition monitoring, acoustic emission, neural networks.

INTRODUCTION

We have obtained acoustic emission (AE) RMS signals from the cylinder liner and cover of the electronically controlled 2-stroke at MAN B&W Research Copenhagen. During the acquisition the running speed was approximately in the range 70-125 rotations per minute. Further, the running speed was virtually constant during periods of constant load settings.

Up to now research has mainly focused on condition monitoring under fixed operational conditions, see further [1], [2] and [3]. We are currently pursuing non-stationary condition monitoring, i.e. condition monitoring under different load settings that should resemble realistic marine conditions. Electronically controlled engines can change the angular timing of certain events, such as fuel injection in order to optimize its performance. However, this behaviour inhibits our framework presented in COMADEM 2003 [1] from detecting condition changes across those load changes. The result is a false alarm triggered by the condition change. Also, mechanically controlled engines display such variations

[4], due to the fact that some events have fixed length in time and some in angular "time". Thus, it is not sufficient to use the crank angular domain as described in [5] to overcome this problem.

This is illustrated in Figure 1. The three events depicted in Figure 1 are believed to arise from mechanical interaction between the injector spindles and their respective stops within the injector, with fuel delivery occurring between the region encompassing the first and second peaks and the last peak. The process is partly mechanically controlled by pre-set spring pressures and partly electronically controlled since the fuel flow to the injector is electronically governed. In order to meet an increased load the engine response is to inject more fuel. This is achieved by prolonging the fuel delivery period with consequential retarded closure of the injector. Since the AE directly reflects the mechanical operations within the injector the increased fuel injection duration is readily identifiable.

Previously, we have presented at event alignment framework, where the different events, e.g. combustion and ignition, are aligned to a reference signal in the crank angle domain [6]. Although this method works well in practice, the alignment is based on landmarks that are found by visual inspection, as seen in Figure 1, which is tedious and time consuming. Note that each example in the crank angle domain has typically 1024/2048 dimension and a large number of events which need to be aligned. This leads to the approach discussed in this paper, where we align an extracted feature instead of the AE patterns in the crank angle domain. Although we only use one feature here, it may easily be expanded to multiple features.

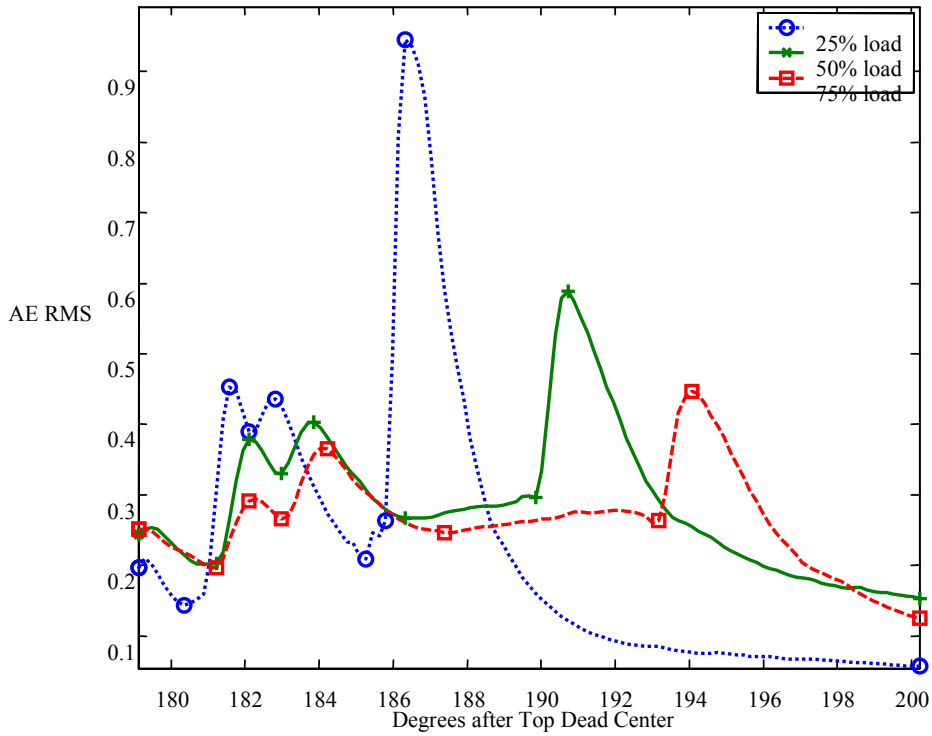

Figure 1: Mean Acoustic emission signals during injection period with different load settings. The markers show the time position of the landmarks that should be aligned. Notice that the TDC refers to another cylinder 180˚ degrees out of phase.

DATA ACQUISITION

The engine is equipped with AE sensors (ultrasonic, 100 kHz – 1 MHz). Further, the engine is equipped with tachometer that allows for sampling in the crank angular domain with a resolution of 1024 samples per revolution. Also, the sample-rate is lowered considerably from 2MHz to 20 kHz, by use of analogue root mean squaring (RMS), thus the data becomes non-negative. Simultaneously, we obtained a 20 kHz signal containing the top dead center (TDC), where the flank indicates when a new engine cycle begins. By summing over the AE RMS signal between the TDC pulses, we obtain a single AE feature for each engine period. Note that this feature is to some extent related to the emitted AE energy of an engine period.

The data acquired has two engine conditions obtained with varying loads on the propeller curve; normal condition with normal lubrication and faulty condition with no lubrication. The normal condition data is obtained at 20%, 25%, 40%, 50%, 60%, 75%, 80%, and 100% load, that on the propeller curve correspond to the running speed of approximately 72, 78, 91, 98, 103, 112, 114 and 123 rounds per minute (RPM). The data for the fault condition is obtained at 25%, 50%, 75% and 100% load.

Figure 2 shows clearly that the faulty condition may easily be detected with the AE feature, as the fault clearly increases the emitted AE energy of the engine. Figure 2 upper panel shows the histogram of AE feature with normal and fault data at 25% load, and lower panel at 50% load. We see that the AE feature discriminates easily between the normal and fault condition, but the AE feature value increases as the load has increased. The fault data at 25% load coincides with normal data at 50% load, thus a simple detection with e.g. a single threshold is not possible.

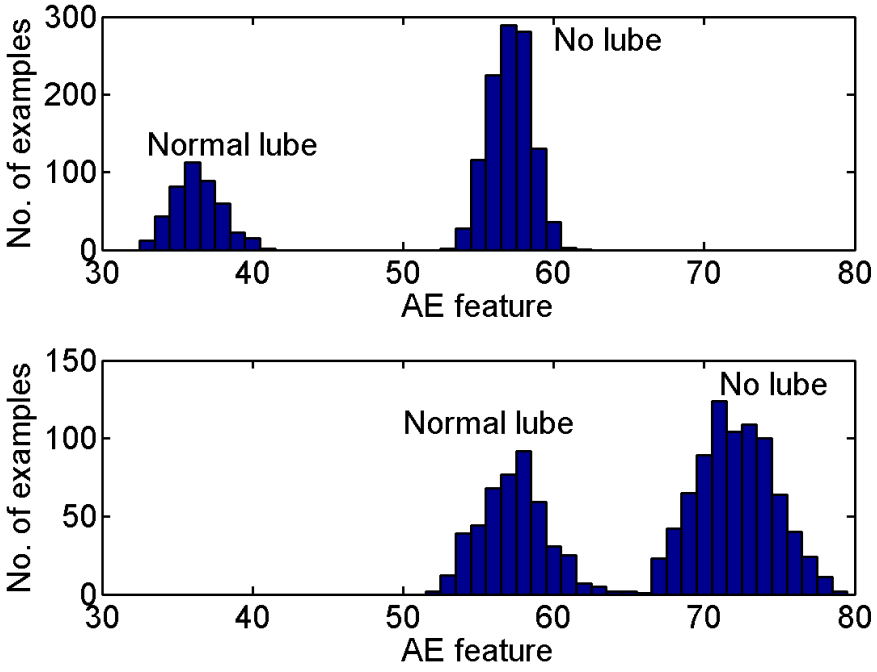

Figure 2: Histogram of AE feature for data with normal lubrication and no lubrication. Upper panel is at 25% load and lower panel at 50% load.

Figure 3 shows the scatter plot of the AE feature vs. the load in RPM for normal and faulty examples. The figure shows that the relation between them is nonlinear, but that the combination of these variables may easily be used for discrimination between normal and fault condition at different loads. We will now describe the supervised and unsupervised methods for modelling this non-linear relation.

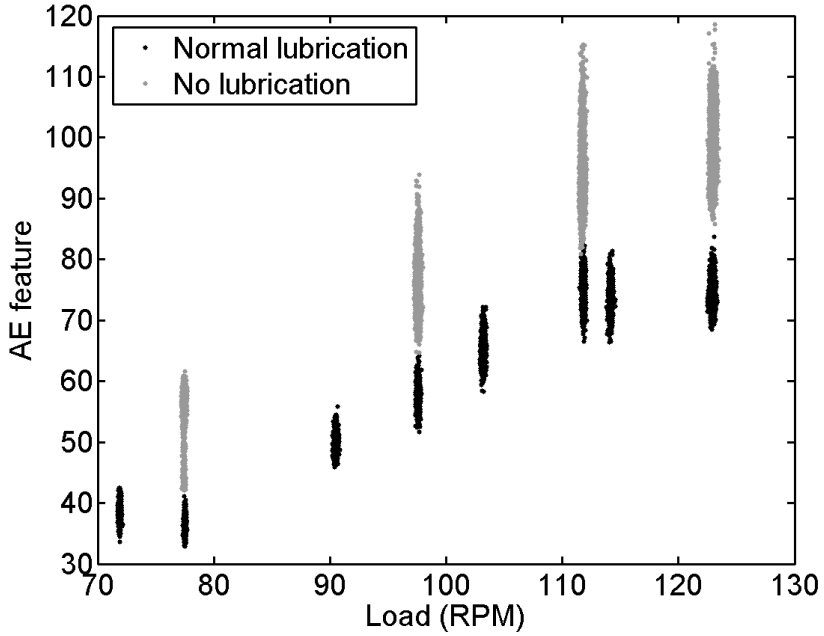

Figure 3: A scatter plot of the AE feature vs. load measured in RPM. The black dots are examples with normal lubrication and the grey dots are examples with no lubrication.

SUPERVISED MODELLING

In a supervised setup, we are interested in modelling the posterior $P(C_{fault} \mid x)$, $0 \le P(C_{fault} \mid x) \le 1$, i.e. the probability of fault given an input pattern $x = [z, l]$, where z is the AE feature and l is the load in RPM. The data set is given by the output/input relations $D = \{t(n), x(n)\}$ where $n = 1, \ldots, N$ and $t(n) = 1$ if the example is faulty and $t(n) = 0$ otherwise. A well established model for non-linear classification is the evidence framework for classification networks [7]. This framework uses feed-forward neural networks with a logistic function output to estimated posterior probability, given by $\hat{P}(C_{fault} \mid x)$. As this type of neural networks is extremely flexible, regularization in the form of weight-decay is applied to constrain the complexity of the network. The amount of regularization is controlled with the evidence framework. For details see [7].

Figure 4 illustrates the estimated posterior of supervised model, where we have used all data for modelling. The solid line indicates the decision boundary at $\hat{P}(C_{fault} \mid x) = 0.5$, given that the cost of misclassification is equal for both classes. The dotted and dashed lines indicate $\hat{P}(C_{fault} \mid x) = 0.1$ and $\hat{P}(C_{fault} \mid x) = 0.9$, respectively. A odd behaviour of the classifier may be noticed at low load. This is due to lack of fault examples at 20% load (at approximately 72 RPM).

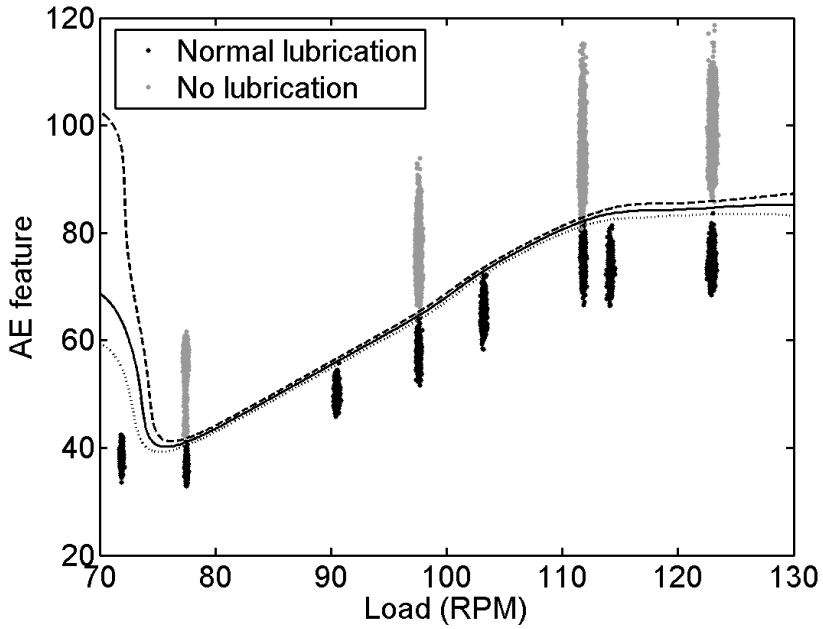

Figure 4: The result of supervised training of all data, using the AE feature and load in RPM as inputs. The solid line indicates the decision boundary between the examples with normal lubrication and no lubrication, i.e. where $\hat{P}(C_{fault} \mid x) = 0.5$. The dotted and dashed line indicate $\hat{P}(C_{fault} \mid x) = 0.1$ and $\hat{P}(C_{fault} \mid x) = 0.9$, respectively.

The performance of the supervised model was evaluated using a cross-validation scheme, where one load with fault is left out and trained on all other loads, in all 4 loads. This procedure was repeated 10 times for each load, by initializing the model differently each time. The performance is visualized as a confusion matrix in Table 1. The results show that 99.8% and 91.2% of the normal and faulty examples are classified correctly, respectively. The false alarm rate is only 0.2%, which is very good, taken in account that the model is classifying examples from a load condition it has not been trained on.

Supervised	Normal lube	No lube
Normal lube*	99.8%	8.8%
No lube*	0.2%	91.2%

Table 1: The confusion matrix for the supervised model on a test set, where * indicates model prediction.

UNSUPERVISED MODELLING

In an unsupervised setup, we only have access to data with normal condition, i.e. no fault examples are used for modelling. In contrast to the supervised approach, we estimated the conditional probability density of the AE feature *z* given the load *l*. The data set is given by the output/input relations $D = \{z(n), l(n)\}$ where $n = 1, \ldots, N$ .We suggest a simple Gaussian conditional probability density given by

$$p(z \mid \mu(l), \sigma^2) = \frac{1}{\sqrt{2\pi}\sigma} \exp\left(-\frac{1}{2\sigma^2}(z - \mu(l))^2 \right)$$

where the mean $\mu(l)$ is a function of the load, while the variance σ^2 is constant. Keeping the variance constant is for computational reasons, as we can observe in Figure 4 that the variance slightly increases proportional to the load. The model can be extended to estimate the variance as a function of the load. To estimate the non-linear mean $\mu(l)$ we use the evidence framework for feed-forward neural networks [8]. In the same way as before, the complexity of the network in constrained by weight-decay regularization, and the amount of regularization is controlled with the evidence framework. By using the evidence framework, we also obtain an estimate of the variance. For details see [8].

Figure 5 shows the results for the unsupervised modelling, using all data for training. The solid line indicates the estimated mean $\hat{\mu}(l)$ and the dashed lines indicate the $3\hat{\sigma}$ distance from the estimated mean. The region between the dashed lines outlines the region where the examples are assumed normal, while examples outside this region are considered faulty. Note that this will introduce a baseline false alarm rate.

The performance of the unsupervised model was evaluated using the same specified data as used to train the supervised model. The performance is visualized as a confusion matrix in Table 2. The results show that 98.5% and 95.6% of the normal and faulty examples are classified correctly, respectively. Compared to the supervised model, the increase in fault detection is on the cost of more false alarms, which is at 1.5%. The false alarms may be reduced by using a time window of examples and applying a binomial hypothesis test, assuming that false alarms on normal examples occur independently in time.

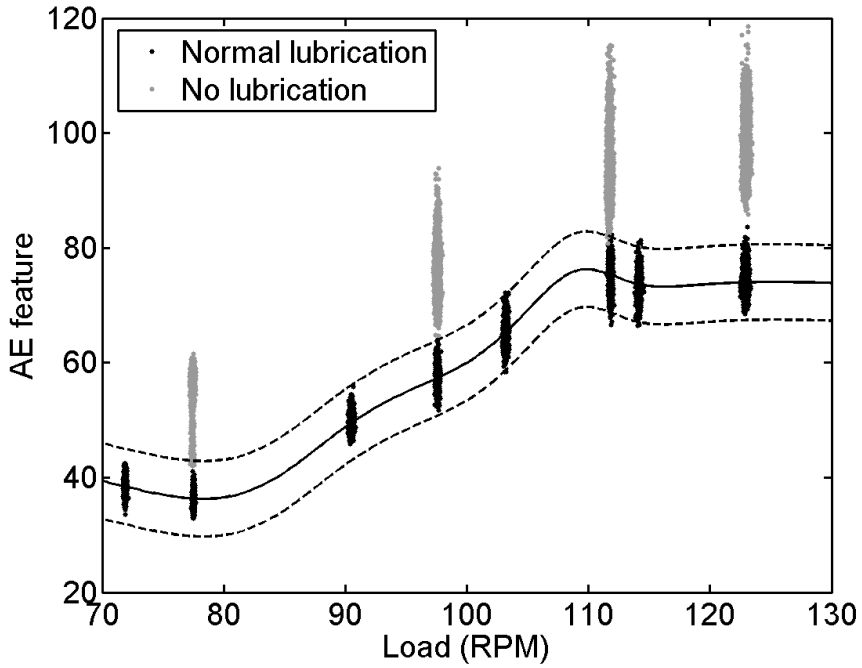

Figure 5: The result of unsupervised training of all normal data, using load in RPM as input and the AE feature as output. The solid line indicates the average AE feature value and dashed lines are three times the estimated standard deviation of the feature.

Unsupervised	Normal lube	No lube
Normal lube*	98.5%	4.4%
No lube*	1.5%	95.6%

Table 2: The confusion matrix for the unsupervised model on a test set, where * indicates model prediction.

CONCLUSION

We have demonstrated a fully automatic non-stationary condition monitoring system. Non-stationarity is a key component in our research for reliable condition monitoring under marine conditions. By applying non-linear models, it is possible to interpolate between different load conditions, thus making it possible to detect faults at unknown load conditions. Moreover, we show that accurate fault detection is possible using only normal data for modelling.

ACKNOWLEDGEMENTS

The work is supported by EU Competitive and Sustainable Growth Programme GRD2-2001-50014 – the AE-WATT project. Data was provided by MAN B&W Diesel A/S.

REFERENCES

[1] Pontoppidan, N. H., Larsen, J., Fog, T., "Independent component analysis for detection of condition changes in large diesels" in COMADEM 2003, no. 16, pp. 493-502, 2003.

[2] Chandroth, G., Sharkey, A. and Sharkey, N., "Vibration signatures, wavelets and principal components analysis in diesel engine diagnostics" in Marine Technology ODRA 99, Oct. 1999.

[3] Fog T., Hansen, L., Larsen, J., Hansen H., Madsen, L., Sørensen, P., Hansen, E. and Pedersen, P., "On Condition Monitoring of Exhaust Valves in Marine Diesel Engines," in Y. H. Hu, J. Larsen, E. Wilson and S. Douglas (eds.), Proceedings of the IEEE Workshop on Neural Networks for Signal Processing IX, IEEE, Piscataway, New Jersey, 1999, pp. 225–234.

[4] Frances A., Gill J., Reuben J. and Steel J., "A Study of the Variability of Acoustic Emission Signals from a Medium Size Marine Diesel Engine under Service Conditions," in O. P. Shrivastav, B. Al-Najjar and R. B. Rao (eds.), COMADEM 2003, COMADEM International, 2003, pp. 503–512.

[5] Chandroth G. and Sharkey A. Utilising the rotational motion of machinery in a high resolution data acquisition system. In Proc of Computers and ships- from ship design and build, through automation and management and on to ship support, May 1999.

[6] Pontoppidan, N. H. and Douglas, R., "Event alignment, warping between running speeds", in COMADEM 2004, pp. 621-628, 2004.

[7] MacKay D.J.C., The Evidence Framework Applied to Classification Networks, "Neural Computation", 1992, Vol. 4, Number 5, pp. 720-736.

[8] MacKay D.J.C., A Practical Bayesian Framework for Backpropagation Networks, "Neural Computation", 1992, Vol. 4, Number 5, pp. 448-472.